Available online at www.sciencedirect.com
ScienceDirect
Trans. Nonferrous Met. Soc. China 27(2017) 102−109
Transactions of Nonferrous Metals Society of China
www.tnmsc.cn

Effect of La on arc erosion behaviors and oxidation resistance of Cu alloys

Hai-yan LI[1], Xuan ZHOU[2], Xue-qiong LU[1], Ya-ping WANG[1,3]

1. Key Laboratory for Nonequilibrium Synthesis and Modulation of Condensed Matter, Ministry of Education, School of Science, Xi'an Jiaotong University, Xi'an 710049, China;
2. Department of Electrical and Computer Engineering, Kettering University, Flint, MI-48504, USA;
3. State Key Laboratory for Mechanical Behavior of Materials, Xi'an Jiaotong University, Xi'an 710049, China

Received 31 December 2015; accepted 18 October 2016

Abstract: Cu with and without La addition was prepared and the effect of a trace amount of La on the arc erosion behaviors and oxidation resistance of Cu alloys was investigated. The results indicate that CuLa alloy exhibits superior oxidation resistance and arc erosion resistance. The contact resistance and temperature rise were obviously improved. The oxidation resistance of CuLa alloy mainly is due to the interface wrapping of La_2O_3 particles and CuLa alloy phase on Cu atoms. Thermodynamic calculation indicated that La_2O_3 could form preferentially in the CuLa alloy, which was beneficial for the protection of the Cu substrate. According to kinetics analysis, the activation energy of CuLa alloy was higher than that of pure Cu, indicating the better oxidation resistance of CuLa alloys.

Key words: CuLa alloy; arc erosion; contact resistance; oxidation; interface wrapping

1 Introduction

Nowadays, the contact materials in low-voltage devices are mainly silver-based materials, such as AgMeO materials [1,2]. The $AgSnO_2$ with various additives are widely considered to be substitutes for AgCdO [3,4]. However, it has been found that the contact resistance and the temperature rise of $AgSnO_2$ are higher than those of AgCdO in the same conditions, which results in limited applications in low-voltage devices [5].

Copper, which is cheaper and more reliable, is a potentially ideal substitute for silver for contact materials used in switching devices such as contactors, circuit breakers and relays [6,7]. However, one of the disadvantages of copper is the poor oxidation resistance in air [8]. Cu-based contacts are easily oxidized under arc and high resistance oxide layers are consequently formed on the surface of the contacts, which result in the contact resistance increasing. This causes acceleration of oxidation of Cu-based contact in turn and even failure of the device [9].

Electrical arc erosion plays a crucial role in the reliability and life of switching devices [10]. Indeed, surface damages resulting from repeated arcing can lead to contact failure under a certain number of operations, i.e., the failure of switching devices is mainly due to contacts welding, contacts destruction, etc [11]. Therefore, a better understanding of the arc erosion behaviors is a key factor in the process of designing Cu-based contacts.

It has been reported that the addition of trace rare earth, such as lanthanum (La), cerium (Ce) and yttrium (Y), and their oxides can improve the oxidation resistance of Cu alloy [12], Mg alloys [13] and other alloys [14,15]. However, there are a few reports about the arc erosion and oxidation behaviors of CuLa alloy. In this work, the mechanism of La effect on the oxidation resistance of the Cu alloy was discussed by the oxidation experiment of CuLa alloys at high temperature and thermodynamic and kinetic analysis.

2 Experimental

2.1 Preparation

The CuLa alloy powders were prepared using vacuum smelting, followed by atomization using

Foundation item: Project (51171146) supported by the National Natural Science Foundation of China
Corresponding author: Ya-ping WANG; Tel: +86-29-82667901; E-mail: ypwang@mail.xjtu.edu.cn
DOI: 10.1016/S1003-6326(17)60011-6

nitrogen gas (N_2). Chemical analysis determined the composition of the atomized powders to be about 0.5% La and 99.5% Cu (mass fraction).

The bulk CuLa alloys were fabricated by typical powder metallurgy methods, including cold pressing at 350 MPa and sintering at 1000 °C for 2 h in vacuum, and then hot pressing at 20 MPa and 800 °C in vacuum.

2.2 Arc erosion experiments

In order to understand the effect of La on the arc erosion behaviors of Cu alloy, the arc erosion experiments have been conducted on the switching devices for several thousands of switching operations. These studies are based on comparison of arc erosion behaviors and pure Cu and CuLa alloy. The Cu and CuLa alloys were processed into *d*6 mm × 6 mm contact for the arc erosion experiments. The contact properties were tested in the following operating conditions, as shown in Table 1. After every 1000 operations, the contact resistance was measured by DC resistance tester, and the temperature rise was measured by Pt100 platinum resistance temperature detector. The microstructure and elementary analysis of the contacts after arcing were carried out using a JSM−7000F field-emission scanning electron microscope (FESEM) operated at 20 kV.

Table 1 Experimental conditions

Parameter	Value
Circuit voltage/V	220
Current/A	8.5
Frequency of operation/min^{-1}	50
Break-make ratio	1:1
Contact force/N	1−9

2.3 Oxidation experiments

The oxidation experiments were carried out to investigate the oxidation behavior of Cu and CuLa alloy in high temperature. The pure Cu and CuLa alloys were machined to *d*10 mm × 5 mm cylinder for the oxidation experiments. High-temperature oxidation was carried out in a muffle furnace in air at 1000 °C for 1 h. The microstructure of the oxide film was observed with a JSM−7000F FESEM, and an energy dispersive spectrometer (EDS) attachment was used to determine the elemental distribution. The oxidation kinetics of pure Cu and CuLa alloys were studied in air using an SDT Q600 simultaneous DSC-TGA instrument with air flow of 50 mL/min. Differential scanning calorimetry (DSC) curve was used to calculate the activation energy. Thermodynamic calculations were performed to predict the primary oxidation occurring on the surface by Gibbs Helmholtz equation [16,17].

3 Results and discussion

3.1 Microstructure of CuLa alloys before and after oxidation

Figure 1 shows the morphologies of CuLa alloy powders. From Fig. 1(a), it can be seen that most of the particles are spherical, with a mean particle size of ~8 μm. Figure 1(b) shows details from Fig. 1(a). The irregular particles in Fig. 1(b) are La-rich phase.

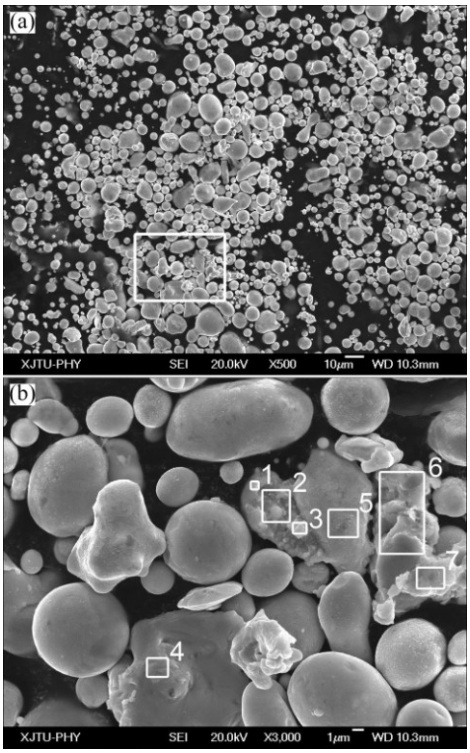

Fig. 1 SEM images of CuLa alloy powders: (a) Morphology of CuLa alloy powders; (b) Details from Fig. 1(a)

Zones 1 and 3 in Fig. 1(b) are CuLa alloy phase, zones 2, 6 and 7 are Cu-rich phase with a relatively high proportion of La, by which zone 5 is surrounded, as shown in Table 2. This indicates that CuLa alloy phase gathers around the Cu phase. Zone 4 in Fig. 1(b), on the other hand, shows a Cu-rich phase with only trace amounts of La.

Table 2 Composition distribution in different zones in Fig. 1 (mass fraction, %)

Zone	O	Cu	La
1		27.47	72.53
2	22.09	37.06	40.85
3		72.53	27.47
4	2.56	93.05	4.39
5		100.00	
6	10.47	78.56	10.97
7	6.42	74.89	18.68

Figure 2 shows the microstructures of CuLa alloy before and after oxidation. It is illustrated that La-rich phase distributes on the boundaries of Cu grains in Fig. 2(a). Since the radius of La atoms is much larger than those of Cu atoms, La atoms might distribute in the irregular boundaries, which results in less free energy of in the CuLa alloy.

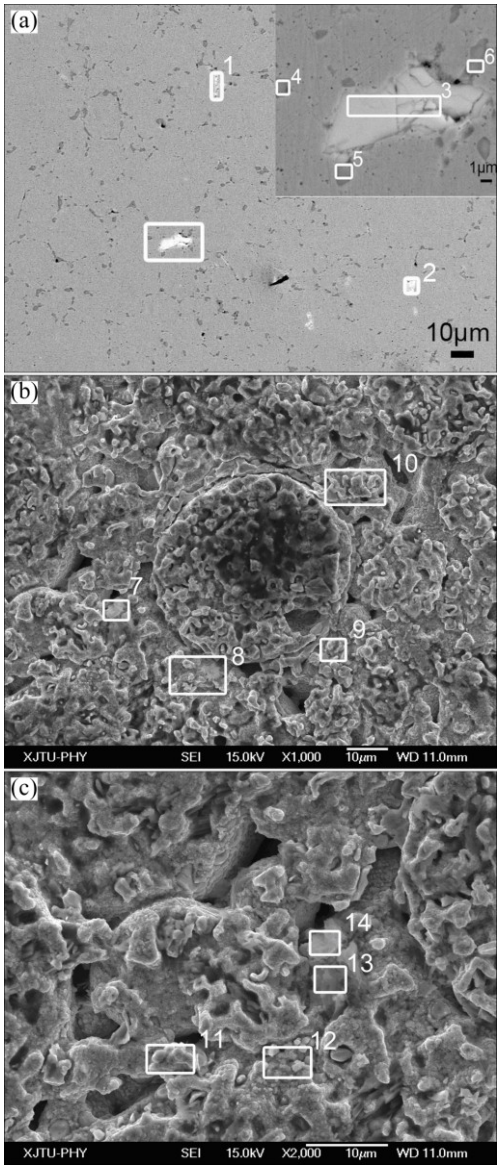

Fig. 2 Microstructures of CuLa alloy: (a) Before oxidation; (b, c) After oxidation

As shown in Table 3, the bright zones (1 and 2) are CuLa alloy phase and zone 3 in inset is La-rich phases, while the gray zones (4, 5 and 6) are Cu-rich phases with a small amount of La. As shown in Table 3, zones 8, 9 and 10 in Fig. 2(b) are Cu-rich phases, while zones 11, 12 and 13 in Fig. 2(c) are La-rich phases. It is considered that oxidation occurs preferentially at the grain boundaries of particles. The active La atoms on the grain boundaries were preferentially oxidized to be La oxide (La_2O_3). La_2O_3 in the interface and CuLa alloy phase wrap the Cu particles, which block the diffusion of oxygen into the Cu matrix and consequently the oxidation resistance is improved.

Table 3 Composition distribution in different zones in Fig. 2 (mass fraction, %)

Zone	O	Cu	La
1		62.46	37.54
2		49.30	50.70
3	2.19	6.80	91.01
4		92.90	7.10
5	0.79	96.13	3.08
6	0.52	98.62	0.85
7	44.65	12.08	43.27
8	19.96	77.31	2.73
9	25.10	74.60	0.30
10	18.42	78.28	3.30
11	12.84	18.56	68.60
12	20.76	12.12	67.12
13	41.35	0	58.65
14	47.37	19.29	33.34

3.2 Effect of La addition on arc erosion behaviors of Cu-based contacts

Figure 3 shows the contact resistance variation of pure Cu and CuLa contacts at different contact forces after several thousands of operations. In the initial stage of switching operation, the contact resistance of Cu contact is slightly higher than that of CuLa contact. However, Fig. 3(a) shows that the contact resistance of pure Cu contacts after 4000 operations is much higher than that after 2000 operations, which is considered to be due to the formation of oxide films and damage of contact surface during the arcing process. The contact resistance of Cu contact is 6 times as high as that of CuLa contact after 5000 switching operations. As a result, the pure Cu contacts fail after about 6350 operations, and the contact resistance is too high to be detected.

As shown in Fig. 3(b), the contact resistance of CuLa contacts is about 30 mΩ at a contact force of 1 N after 10000 operations, but it decreases to about 18 mΩ when the contact force is 3 N. The decrease in contact resistance results from initial cracking of the oxide film and increase of the practical contact area. Then, the contact resistance decreases to 9 mΩ with a max contact force 9 N, which is due to extensive fracturing of the oxide film. It is concluded that oxide film of the CuLa contact can be fractured by increasing the contact force and the contact resistance is reduced.

Figure 4 shows the temperature rise variation of pure Cu and CuLa contacts at different contact forces

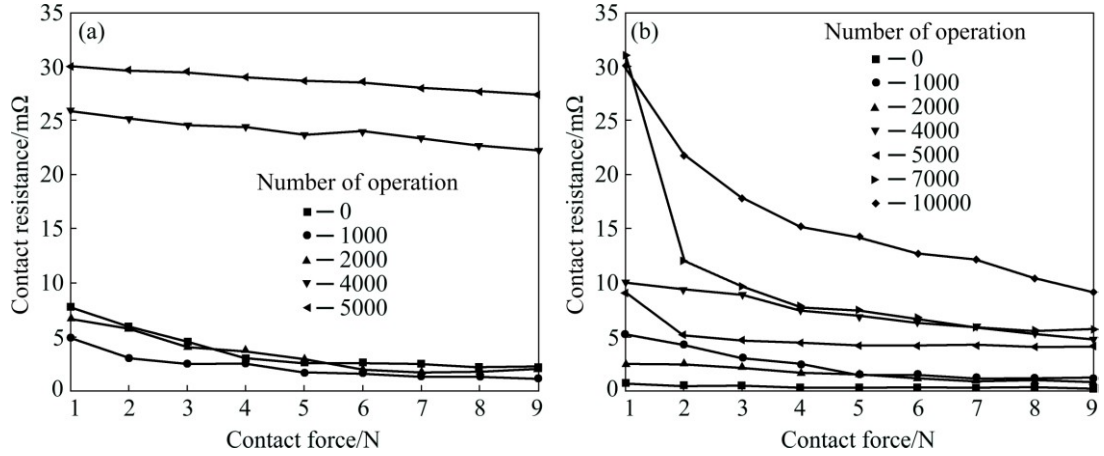

Fig. 3 Curves of contact resistance versus contact force after switching operations: (a) Pure Cu contacts; (b) CuLa contacts

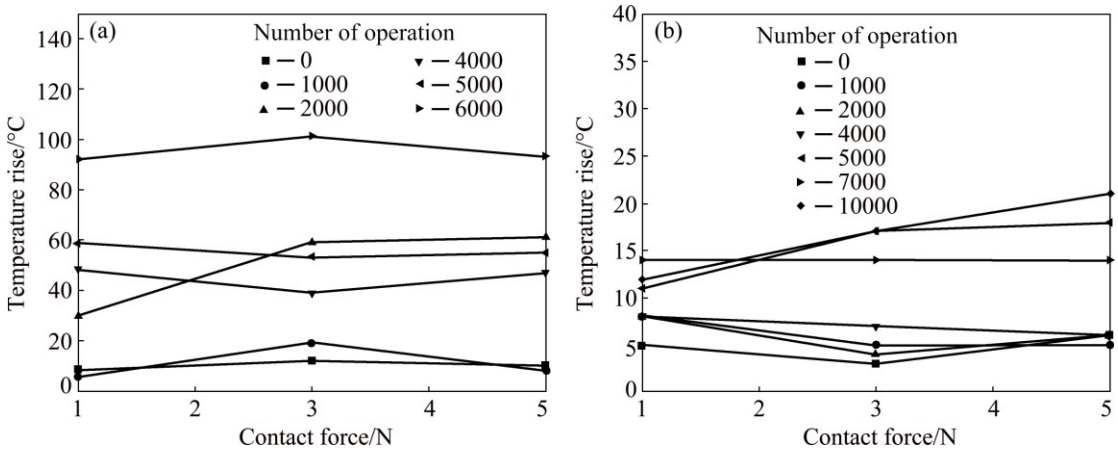

Fig. 4 Curves of temperature rise versus contact force after switching operations: (a) Pure Cu contacts; (b) CuLa contacts

after several thousands of switching operations. As shown in Fig. 4(a), the temperature rise of pure Cu contacts at initial stage is about 10 °C at 5 N and increases up to 60 °C after 2000 switching operations, finally reaches 90 °C after 6000 operations. The rapid temperature rise is related with the increased contact resistance shown in Fig. 3, which results in localized joule heating and can cause a considerable increase in the localized temperature and growth of oxide film on the contact surface.

Figure 4(b) shows that the temperature rise of CuLa contacts is 5 °C after 2000 operations and 20 °C after 10000 operations at 5 N. The temperature rise increases slowly and is significantly reduced by the addition of La.

The surface morphologies of the movable contact after switching operations are shown in Fig. 5. Several big mounds and craters are observed after 6350 operations for pure Cu contacts as shown in Figs. 5(a) and (b). The pure Cu contacts suffer concentrated arc erosion. The big mounds are as a result of the drag of electromagnetic forces induced by the electrical arc, and the large eroded crater is formed because of serious sputter and materials transfer. This serious surface damage finally results in contact failure after about 6350 operations. While the surface of CuLa contact is much smoother than that of pure Cu and only some small bulges and craters formed after 10000 operations. Figure 5(d) gives a magnified view of Fig. 5(c). The area is filled up or covered by the molten metal during solidification. The addition of trace La therefore improves the surface morphology and increases the life of the contact.

Table 4 shows that zones 1 and 2 are Cu-rich phases with a small amount of La element, which may be CuLa alloy and La_2O_3. La_2O_3 with high temperature stability and good wettability is formed under arc. Thus, suspended La_2O_3 in the Cu molten pool increases the viscosity and reduces arc erosion by reducing the spattering of liquid Cu. Therefore, the addition of La improves the arc erosion resistance of the contact.

3.3 Kinetics of oxidation of CuLa alloy

The kinetics of oxidation are conducted to calculated the activation energy. Figures 6(a) and (b) show the DSC curves of pure Cu and CuLa alloy fragments with different heating rates, respectively. The

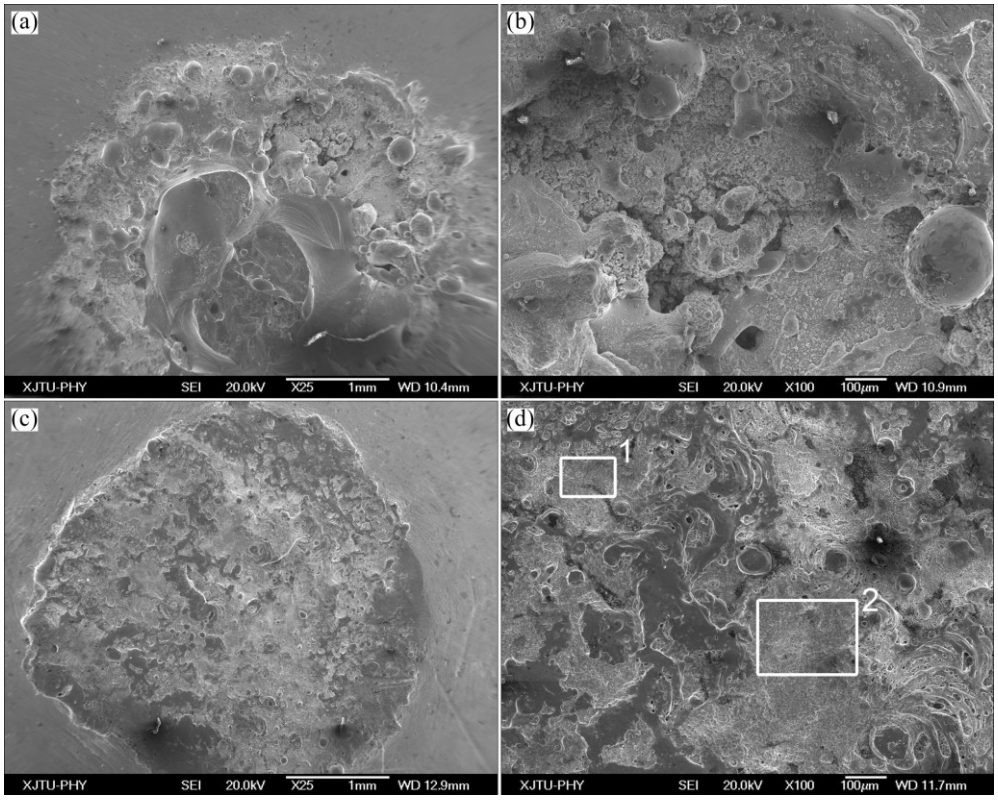

Fig. 5 Surface morphologies of movable contact of pure Cu after 6350 operations (a, b) and CuLa after 10000 operations (c, d)

Table 4 Composition distribution in different zones in Fig. 5 (mass fraction, %)

Zone	O	Cu	La
1	28.48	71.08	0.44
2	9.05	89.73	1.21

obvious peak range from 800 to 1000 °C is where oxidation mainly occurs.

The variation of the peak temperatures with heating rates can be used to determine the oxidation activation energy according to Kissinger equation:

$$\ln(\beta/T_p^2)=\ln(AR/E)-(E/R)\cdot(1/T_p) \quad (1)$$

where β is the heating rate, T_p is the peak temperature at a given heating rate, E is the activation energy, R is the gas constant and A is the pre-exponential factor. The oxidation activation energy of CuLa alloys is determined as 172.16 kJ/mol. The oxidation activation energy of pure Cu is determined as 133.13 kJ/mol. The activation energy of CuLa alloys is higher than that of pure Cu, indicating the superior oxidation resistance of CuLa alloys.

3.4 Thermodynamic calculation of oxidation of CuLa alloy

According to the thermodynamic theory [18], the following reactions might take place:

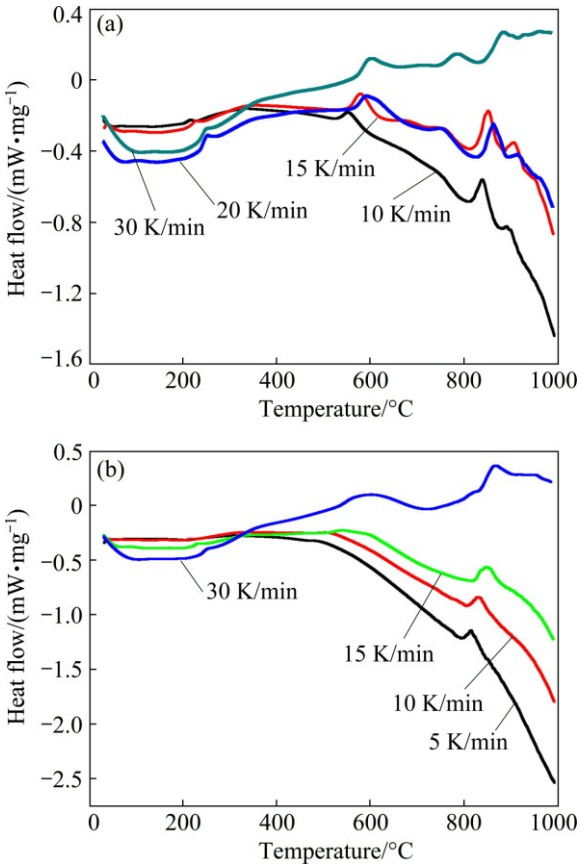

Fig. 6 DSC curve of Cu and CuLa alloy at different heating rates: (a) Pure Cu; (b) CuLa alloys

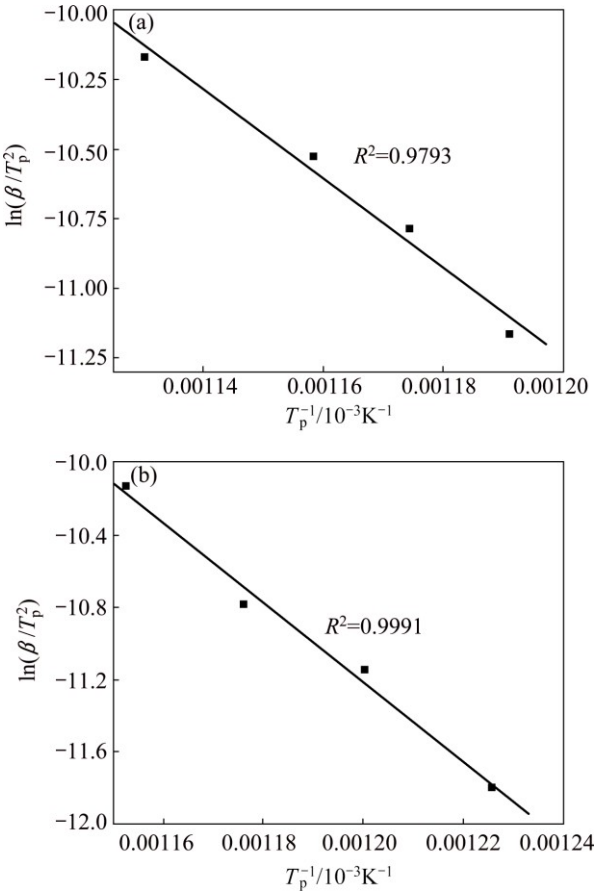

Fig. 7 Plots of $\ln(\beta/T_p^2)$ versus $1/T_p$ of pure Cu (a) and CuLa (b) alloys

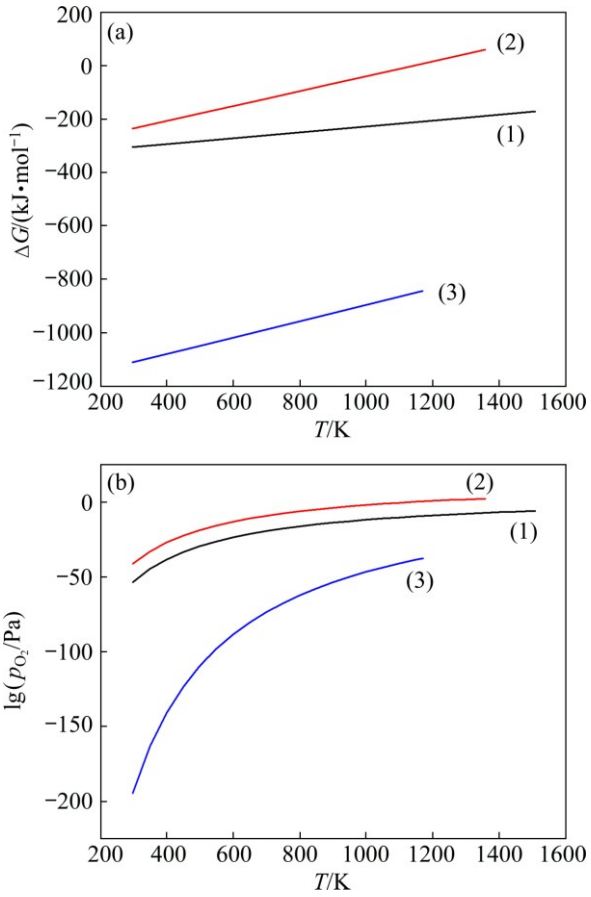

Fig. 8 Relationship between Gibbs free energy ΔG and temperature (a) and relationship between $\lg p_{O_2}$ and temperature for formation of different oxides (b)

$$4Cu+O_2=2Cu_2O \quad (2)$$

$$2Cu+O_2=2CuO \quad (3)$$

$$(4/3)La+O_2=(2/3)La_2O_3 \quad (4)$$

The Gibbs free energies of Eqs. (2), (3) and (4) can be calculated by thermodynamic parameters [18−20], and the results are shown in Fig. 8(a). These three reactions of oxidation can occur spontaneously in thermodynamics because the values of ΔG are negative. It can been clearly seen from Fig. 8(a) that the oxidation of La is the easiest one to occur spontaneously thermodynamically due to the lowest ΔG value in these three reactions. The oxide with higher to lower thermodynamic stability is sequenced as La_2O_3>Cu_2O> CuO.

According to Gibbs' function [18], oxygen partial pressures of oxidation of CuLa alloy are calculated by Eqs. (2), (3) and (4) and thermodynamic condition diagram of oxidation is obtained and shown in Fig. 8(b). Figure 8(b) shows that oxygen partial pressure of La oxidation is very low and there is a large area of preferential oxidation. Therefore, the preferential oxidation of CuLa alloy is feasible thermodynamically.

3.5 Model of interface wrapping of La effect on oxidation resistance of CuLa alloy

The model of La effect on the oxidation resistance of Cu alloy is shown in Fig. 9. As shown earlier in Fig. 1 and Fig. 2, La atoms and CuLa alloy phase mainly distribute at the irregular grain boundaries of Cu alloys. Since active La atoms are more easily oxidized than Cu atoms at high temperature, La atoms on the boundaries are preferably oxidized and La_2O_3 forms around the grain boundaries. Some Cu atoms are thus entirely wrapped by La_2O_3 particles, as illustrated in Fig. 9(a), and the inward diffusion of oxygen and outward diffusion of Cu atoms is blocked to some extent, which reduces the oxidation rate of the alloys. In addition, some Cu atoms are locally wrapped by CuLa alloy phase, as shown in Fig. 9(b), the effect of La on oxidation resistance and arc erosion is reduced. But it somewhat reduces chance of Cu atoms contacting with oxygen atoms and the overall oxidation resistance is still much greater than that of pure Cu. So, the combined effect of both entire and local interface wrapping of La on the Cu atoms contributes to the improvement of the oxidation resistance of Cu alloy.

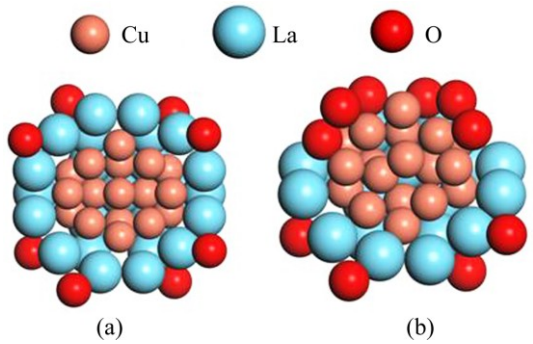

Fig. 9 Model of oxidation of CuLa alloy: (a) Entirely wrapping; (b) Locally wrapping

4 Conclusions

1) CuLa alloys exhibited better oxidation resistance and arc erosion resistance than pure Cu. It was found that the contact resistance of CuLa contacts after 10000 operations was lower and more stable than that of pure Cu after 5000 operations. The temperature rise of pure Cu contacts was close to 90 °C after 6000 operations, whereas the temperature rise of CuLa contacts was only 20 °C after 10000 operations. Furthermore, the eroded surface of pure Cu contacts exhibited large craters and serious eroded morphology, finally resulting in the pure Cu contacts failing after about 6350 operations.

2) Thermodynamic calculation indicated that La element was more favorable to react with oxygen and La_2O_3 formed preferentially in the CuLa alloy. The better oxidation resistance of CuLa alloy than pure Cu was confirmed according to kinetics analysis.

3) The oxidation resistance of CuLa alloys mainly attributed to the entire interface wrapping of La_2O_3 particles on Cu atoms and the local interface wrapping of CuLa alloy phase on Cu atoms.

References

[1] BEHRENS V, HONIG T, KRAUS A, MICHAL R, SAEGER K E, SCHMIDBERGER R, STANEFF T. An advanced silver/tin oxide contact material [J]. IEEE Transactions on Components, Packaging, and Manufacturing Technology, Part A, 1994, 17(1): 24−31.

[2] XU Cai-hui, YI Dan-qing, WU Chun-ping, LIU Hui-qun, LI Wei-zhou. Microstructures and properties of silver-based contact material fabricated by hot extrusion of internal oxidized Ag−Sn−Sb alloy powders [J]. Materials Science and Engineering A, 2012, 538: 202−209.

[3] VERMA P, PANDEY O P, VERMA A. Influence of metal oxides on the arc erosion behavior of silver metal oxides electrical contact materials [J]. Journal of Materials Science and Technology, 2004, 20(1): 49−52.

[4] ĆOSOVIĆ V, ĆOSOVIĆ A, TALIJAN N, ŽIVKOVIĆ D, MINIĆ D. Improving dispersion of SnO_2 nanoparticles in Ag−SnO_2 electrical contact materials using template method [J]. Journal of Alloys and Compounds, 2013, 567: 33−39.

[5] VERMA P, PANDEY O P, VERMA A. Influence of metal oxides on the arc erosion behaviour of silver metal oxides electrical contact materials [J]. Journal of Materials Science and Technology, 2004, 20(1): 49−52.

[6] CUI Y S, WANG Y, SHAO W Z, ZHEN L, IVANOV V V. Microstructure analysis and the effect of Cr additive on the electrical performance of (Cp−Nb)/Cu−Cd electrical contact materials [C]//Proceedings of the 52th IEEE Holm Conference on Electrical Contacts. Canada: Montreal IEEE, 2006: 136−142.

[7] GÜLER Ö, EVIN E. The investigation of contact performance of oxide reinforced copper composite via mechanical alloying [J]. Journal of Materials Processing Technology, 2009, 209(3): 1286−1290.

[8] SHAO Wen-zhu, ZHEN Liang, LI Yi-chun, CUI Yu-sheng, ZHOU Jin-song. Oxidized film on Cp/Cu−Cd electrical contact material [J]. Transactions of Nonferrous Metals Society of China, 2005, 15(2): 251−255.

[9] LIU P, BAHADUR S, VERHOEVEN J D, GIBSON E D, KRISTIANSEN M, DONALDSON A. Arc erosion behavior of Cu−15% Nb and Cu−15%Cr in situ composites [J]. Wear, 1997, 203: 36−45.

[10] CHEN Z K, MIZUKOSHI H, SAWA K. Contact erosion patterns of Pd material in DC breaking arcs [J]. IEEE Transactions on Components, Packaging, and Manufacturing Technology: Part A, 1994, 17(1): 61−67.

[11] CHEN Z K, SAWA K. Polarity effect of unsymmetrical material combination on the arc erosion and contact resistance behavior [J]. IEEE Transactions on Components, Packaging, and Manufacturing Technology: Part A, 1995, 18(2): 334−343.

[12] MU Zhen, GENG Hao-ran, LI Meng-meng, NIE Guang-lin, Leng Jin-feng. Effects of Y_2O_3 on the property of copper based contact materials [J]. Composites (Part B): Engineering, 2013, 52: 51−55.

[13] YU Xiao-wen, SHEN Shi-jun, JIANG Bin, JIANG Zhong-tao, YANG Hong, PAN Fu-sheng. The effect of the existing state of Y on high temperature oxidation properties of magnesium alloys [J]. Applied Surface Science, 2016, 370: 357−363.

[14] ZHAO Shi-zhe, ZHOU Hong, ZHOU Ti, ZHANG Zhi-hui, LIN Peng-yu, REN Lu-quan. The oxidation resistance and ignition temperature of AZ31 magnesium alloy with additions of La_2O_3 and La [J]. Corrosion Science, 2013, 67: 75−81.

[15] MENG Jun-sheng, JI Ze-sheng. Effect of La_2O_3/CeO_2 particle size on high-temperature oxidation resistance of electrodeposited Ni−La_2O_3/CeO_2 composites [J]. Transactions of Nonferrous Metals Society of China, 2014, 24(11): 3571−3577.

[16] WU Chun-ping, YI Dan-qing, CHEN Jing-chao, LI Jian, LIU Hui-qun, WANG Bing, FANG Xi-ya. Internal oxidation thermodynamics and microstructures of Ag−Y alloy [J]. Transactions of Nonferrous Metals Society of China, 2007, 17: 262−266.

[17] FAN J F, YANG Ch L, HAN G, FANG S, YANG W D, XU B S. Oxidation behavior of ignition-proof magnesium alloys with rare earth addition [J]. Journal of Alloys and Compounds, 2011, 509: 2137−2142.

[18] YE D L. Practical thermodynamics data manual of inorganic matters [M]. Beijing: Metallurgical Industry Press, 1981. (in Chinese)

[19] KONINGS R J M, BENEŠ O. The thermodynamic properties of the *f*-elements and their compounds. I. The lanthanide and actinide metals [J]. Journal of Physical and Chemical Reference Data, 2010, 39(4): 1−47.

[20] NAVROTSKY A, LEE W, GRYN A M, USHAKOV S V, ANDERKO A, WU H H, RIMAN R E. Thermodynamics of solid phases containing rare earth oxides [J]. The Journal of Chemical Thermodynamics, 2015, 88: 126−141.

La 对铜合金的电弧侵蚀行为和抗氧化性能的影响

李海燕[1]，周 轩[2]，卢雪琼[1]，王亚平[1,3]

1. 西安交通大学 理学院 物质非平衡合成与调控教育部重点实验室，西安 710049；
2. Department of Electrical and Computer Engineering, Kettering University, Flint, MI-48504, USA;
3. 西安交通大学 材料力学行为国家重点实验室，西安 710049

摘 要：研究稀土元素 La 对铜合金的电弧侵蚀行为和氧化行为的影响。结果表明：稀土元素 La 的加入有利于铜合金抗氧化性能和电弧侵蚀性能的改善，并有效地降低了接触电阻和温升。通过对 CuLa 合金的高温抗氧化性能机理分析表明，富集在晶界的 La 元素形成 La_2O_3 或者 CuLa 合金，起到了界面包裹的作用，从而抑制了铜的进一步氧化。通过热力学计算可知，CuLa 合金中的 La 择优氧化形成 La_2O_3，对铜基体起到了保护作用。动力学分析表明，CuLa 合金的激活能较纯铜的高，说明其抗氧化性能更好。

关键词：CuLa 合金；电弧侵蚀，接触电阻；氧化；界面包裹

(Edited by Yun-bin HE)